

Experimental And Numerical Analysis Of Flow Path Change In Rock Fracture Under Hydrothermal Condition

Cite as: AIP Conference Proceedings **987**, 133 (2008); <https://doi.org/10.1063/1.2896959>
Published Online: 29 February 2008

N. Watanabe, H. Iijima, N. Hirano, et al.



View Online



Export Citation



1.8 GHz

8.5 GHz

Trailblazers. New

Meet the Lock-in Amplifiers that measure microwaves.

Zurich Instruments [Find out more](#)

Experimental And Numerical Analysis Of Flow Path Change In Rock Fracture Under Hydrothermal Condition

N. Watanabe, H. Iijima, N. Hirano and N. Tsuchiya

Graduate School of Environmental Studies, Tohoku University, 6-6-20, Aoba, Aramaki, Aoba-ku, Sendai, 980-8579, Japan

Abstract. A hydrothermal flow-through experiment was performed for an artificially created single tensile fracture of granite. Water that had dissolved granite (Si concentration: 250 ppm) was injected into the fracture under hydrothermal conditions (effective normal stress: 10-13 MPa, temperature: 150 °C) during 450 hours. Non-monotonic changes of fracture permeability were observed. Fracture permeability decreased significantly only during first 150 hours. Si concentration of water produced from the fracture was increased monotonically. However, the Si concentration was smaller than that of water injected into the fracture. A numerical modeling using experimental data was also performed for hydrothermal flow in the fracture. Aperture structures for the beginning and the end of the experiment and resulting hydrothermal flow were determined using experimentally obtained fracture surface geometries and fracture permeability. For the beginning of the experiment, developments of preferential flow paths (channeling flow) in heterogeneous aperture structure were observed obviously, while the developments of preferential flow paths were not observed obviously for the end of the experiment. It was also observed that local apertures around the preferential flow paths for the beginning of the experiment tended to become smaller at the end of the experiment, while other local apertures for the beginning of the experiment tended to become greater at the end of the experiment. Although both increase and decrease of local apertures were observed between the beginning and the end of the experiment, arithmetic mean values of local apertures for the end of the experiment (71 μm) was smaller than that for the beginning of the experiment (84 μm).

Keywords: Preferential flow path, rock fracture, flow-through experiment, numerical modeling channeling flow, aperture structure, water-rock interactions

PACS: 91.55.Jk, 91.60.Ba, 91.60.Np, 91.65.My

INTRODUCTION

Since geofluids flow through rock fractures, understanding of flow properties of a rock fracture under various geological conditions is one of the most important factors for understanding of the Earth as a dynamic system. In our recent coupled experimental-numerical studies for water flow through artificially created fractures of granite, channeling flow (developments of preferential flow paths) has been observed in heterogeneous aperture structures of the fractures [1]. It is suggested that channeling flow usually occurs in rock fractures under normal stresses of 10-100 MPa (and, correspondingly, at depths of 400-4,000 m).

Our previous studies proposed a coupled experimental-numerical method for imaging channeling flow in a rock fracture under normal stress and provided fundamental insights of the phenomena. However, it is not clear how (preferential) flow paths

in a rock fracture change by water-rock interactions (dissolution and/or precipitation) under hydrothermal conditions. No experimental observation has been performed for changes of flow paths in a rock fracture under hydrothermal conditions. Previous experimental studies have focused on changes of fracture permeability [2]. A few numerical studies provided information for changes of flow paths in a rock fracture under hydrothermal conditions [3]. However, in the numerical studies, simulations were performed under ideal conditions.

The objective of the present study is to reveal changes of flow paths in a rock fracture under hydrothermal conditions using a coupled experimental-numerical method. A hydrothermal flow-through experiment was performed for an artificially created rock fracture, and hydrothermal flow in heterogeneous aperture structure of the fracture was determined for the beginning and the end of the experiment using a numerical modeling and experimental data.

METHODS

Hydrothermal Flow-through Experiment

A cylindrical rock sample that contains an artificially created fracture is used in a hydrothermal flow-through experiment. The sample is 50 mm in diameter and 120 mm in length and contains a single fracture along the long axis. The sample is also used in measurements of fracture surface geometries at the beginning and the end of the experiment. The fracture is separated into two surfaces, and 2-D distributions of asperity heights are measured for each surface in a 250 μm square grid system (200 \times 480 data points) using a laser-scanning equipment.

An experimental system for a hydrothermal flow-through experiment is shown in Fig. 1. The system was developed using the Rubber-Confining Pressure Vessel [4]. The Rubber-Confining Pressure Vessel (R-CPV) with a sample is placed in a pressing machine (maximum load: 25,000 kg). By controlling the load of the pressing machine, prescribed confining pressure is applied to the sample, where a fracture of the sample is subjected to the same normal stress as the confining pressure. Distilled water (room temperature) is injected into the fracture at a prescribed flow rate via a pre-heating unit using a pump. In the R-CPV, prescribed effective normal stress is applied to the fracture by controlling pore pressure using a pressure-regulating valve, and prescribed temperature is maintained using a heating jacket.

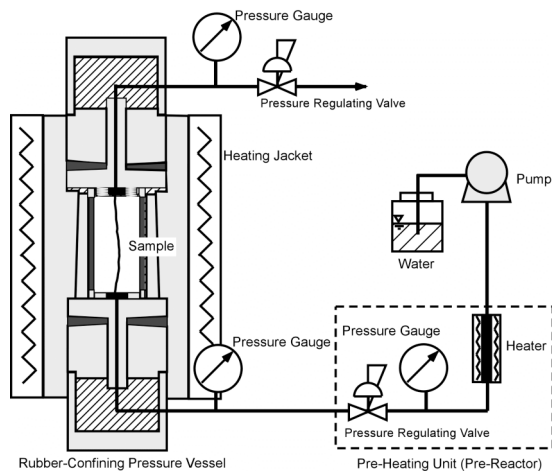


FIGURE 1. Experimental system for the hydrothermal flow-through experiment.

In the experiment, hydraulic pressure difference between inlet and outlet sides of a rock fracture is measured at every prescribed time for evaluation of fracture permeability. Fracture permeability is

calculated on the basis of the cubic law assumption using dimensions of rock fracture, fluid viscosity, hydraulic pressure difference and flow rate (see, Equations (2) and (3) in the next section). In addition, produced water is collected every prescribed times and analyzed using ICP-AES to infer water-rock interactions in a rock fracture.

Numerical Flow Modeling Using Experimental Data

A numerical model, which incorporates experimentally measured fracture surface geometries and fracture permeability, is used for determination of an aperture structure of a rock fracture and hydrothermal flow in the aperture structure. A model of an aperture structure is constructed on a computer by using digital data of fracture surface geometries. The local cubic law (LCL) based hydrothermal flow-through simulation is performed for the model under the same boundary conditions as those in a hydrothermal flow-through experiment. Based on the simulation, the permeability of the model is evaluated using the same equations as those in the flow-through experiment, and the permeability is compared with the experimentally obtained fracture permeability. By matching the numerically obtained permeability with the experimentally obtained permeability through a modification of the model (a simulation of the normal displacement of a rock fracture), an aperture structure and resulting hydrothermal flow are determined.

A model of an aperture structure is represented by a 2-D distribution of local apertures in a 250 μm square grid system, where the local apertures are represented by vertical separations between mean planes of opposite fracture surfaces. A model with at least a single contact point of fracture surfaces is initially constructed, and the model is then modified through a simulation for normal displacement (close) of a rock fracture to match the permeability of a model with experimentally obtained fracture permeability. In the modification, all local apertures are reduced uniformly. Although the deformation of actual fracture surfaces depends completely on stress and temperature conditions, the deformation is neglected except for contacting asperities of the fracture surfaces, because it is expected that the deformation occurred predominantly at these points. In addition, vanishing overlapped contacting asperities simulates both the elastic and permanent deformations of the contacting asperities and created zero local apertures [5].

The 3-D flow of incompressible and viscous fluid (water) through an aperture structure of a rock fracture is approximated by the Reynolds equation for a laminar flow in a 2-D field [6]:

$$\frac{\partial}{\partial x} \left(\frac{e^3}{12\mu} \frac{\partial P}{\partial x} \right) + \frac{\partial}{\partial y} \left(\frac{e^3}{12\mu} \frac{\partial P}{\partial y} \right) = 0, \quad (1)$$

where e is local aperture, μ is fluid viscosity and p is hydraulic pressure.

Liner equations derived from a finite difference form of Equation (1) are solved using a simulator, the D/SC [7], by substituting zero local apertures at contacting asperities with $0.1 \mu\text{m}$ local apertures, and by assuming constant water viscosity, for convenience. Boundary conditions are given such that macroscopic water flow occurred in one direction. The condition of constant pressure (constant macroscopic pressure gradient) is given for boundaries perpendicular to the direction of macroscopic flow, and the condition of non-flow is given for boundaries parallel to the direction of macroscopic flow.

The hydraulic aperture (e_h) is calculated using the following equation [8]:

$$e_h = \left(\frac{12\mu Q}{W(\Delta P/L)} \right)^{1/3}, \quad (2)$$

where Q is flow rate, W and L are the length of the boundaries perpendicular and parallel to the macroscopic flow and $\Delta P/L$ is the macroscopic pressure gradient. In addition, permeability (k) is calculated using the following equation:

$$k = \frac{e_h^2}{12}. \quad (3)$$

RESULTS

A hydrothermal flow-through experiment was performed for a granite sample containing a tensile fracture. Effective normal stress in a fracture plane was 10-13 MPa, where normal stress and pore pressure were 16 MPa and 3-6 MPa, respectively. Temperature and flow rate were $150 \text{ }^\circ\text{C}$ and $120 \mu\text{l}/\text{min}$, respectively. A pipe of pre-heating unit was filled with crushed granite particles (1 mm in diameter), and temperature and hydraulic pressure were $350 \text{ }^\circ\text{C}$ and 20 MPa, respectively. According to our preliminary tests, Si concentration of water injected into the fracture was approximately 250 ppm under the conditions. The experiment was performed during 450 hours. In addition, the numerical modeling using experimental data was performed using data of fracture surface geometries and fracture permeability measured at the beginning and the end of the experiment.

A change of fracture permeability with time is shown in Fig. 2. Fracture permeability was $2.2 \times 10^{-13} \text{ m}^2$ (hydraulic aperture: $1.6 \mu\text{m}$) at the beginning of the experiment, and decreased to $0.26 \times 10^{-13} \text{ m}^2$ (hydraulic aperture: $0.56 \mu\text{m}$) at the end of the experiment. In addition, non-monotonic decrease of fracture permeability was observed. Significant decrease occurred during first 150 hours. On the other hand, gradual decrease occurred during 150-450 hours. Si concentration of produced water increased with time monotonically. However, the concentration was smaller than that of water injected over the experiment.

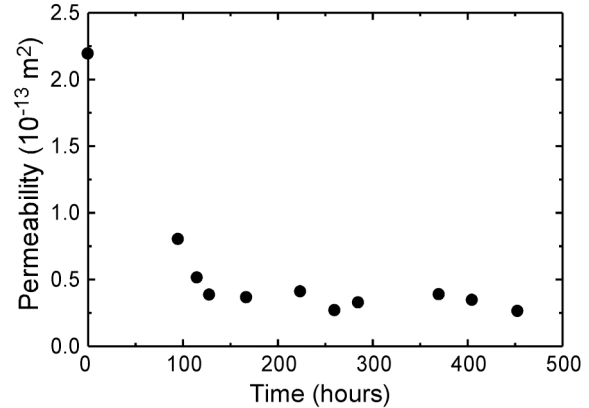


FIGURE 2. Changes of fracture permeability with time in the hydrothermal flow-through experiment for an artificially created tensile fracture of granite.

Images of aperture structures for the beginning and the end of the experiment and hydrothermal flow in the aperture structures are shown in Fig. 3. The images of hydrothermal flow are the distributions of local flow rates that are normalized by the maximum values in each aperture structure. Since the local flow rates ranged from unity to values much smaller than unity, only the relatively greater local flow rates (1-0.001) are indicated by gray scale, and the remaining smaller local flow rates (< 0.001) are indicated in black, as is the case for the local flow rates of 0.001. Comparing the images between the aperture structures and hydrothermal flow, the magnitudes of local apertures did not always correspond to those of the local flow rates for both the beginning and the end of the experiment. For the beginning of the experiment, developments of preferential flow paths (continuous points of relatively high flow rate in limited regions) were obvious. However, significantly different flow paths were observed for the end of the experiment. In addition, development of preferential flow paths was not obvious (particularly in the middle of the image). It was also observed that local apertures around the preferential flow paths for the beginning of the

experiment tended to become smaller at the end of the experiment, while other local apertures for the beginning of the experiment tended to become greater at the end of the experiment. Although both increase and decrease of local apertures were observed between the beginning and the end of the experiment, the arithmetic mean value of local apertures for the end of the experiment (71 μm) was smaller than that for the beginning of the experiment (84 μm).

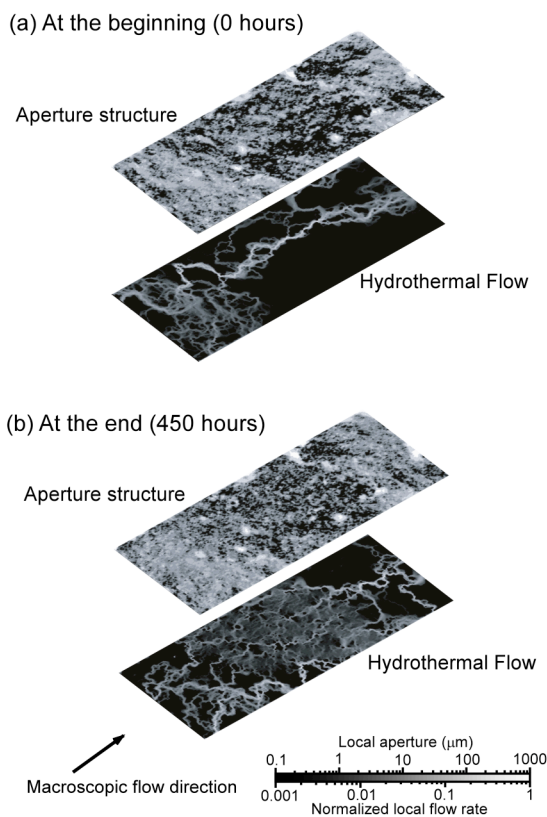


FIGURE 3. Numerically determined aperture structures and hydrothermal flow in the aperture structures for the beginning and the end of a hydrothermal flow-through experiment for an artificially created tensile fracture of granite.

DISCUSSION AND CONCLUSIONS

In the experiment, non-monotonic decrease of fracture permeability with time was observed. Since Si concentration of produced water from the fracture was smaller than that of water injected into the fracture over the experiment, it is expected that mineral precipitation occurred in the fracture. On the other hand, according to the numerical modeling, it was observed that obvious preferential flow paths were developed for the beginning of the experiment, and it was also observed that obvious preferential flow paths decreased for the end of the experiment. Surprisingly,

it is expected that the changes of flow paths were caused by both mineral precipitation and dissolution, since it was observed that local apertures away from preferential flow paths for the beginning of the experiment tended to become greater at the end of the experiment. The coupled experimental-numerical observation indicated complex mechanisms for changes of flow paths in a rock fracture (and, correspondingly, changes of fracture permeability) even under deceptively simple hydrothermal conditions. It is also indicated that channeling flow in a rock fracture can be ceased by long-term water-rock interactions. Further studies are required to reveal changes of flow paths in rock fractures under different conditions and mechanisms of the phenomena.

ACKNOWLEDGMENTS

The authors would like to thank Dr. K. TEZUKA, Dr. T. TAMAGAWA (Japan Petroleum Exploration Co., Ltd.) and Dr. K. WATANABE (Rich Stone Limited) for their assistance in the flow-through simulations with the D/SC.

REFERENCES

1. Watanabe, N., N. Hirano, T. Tamagawa, K. Tezuka and N. Tsuchiya (2005), Numerical estimation of aperture structure and flow wetted field in rock fracture, *Geotherm. Resour. Council Trans.*, 29, 431-436.
2. Polak, A., D. Elsworth, J. Liu and A. S. Grader (2004) Spontaneous switching of permeability changes in limestone fracture with net dissolution, *Water Resour. Res.*, 40, W03502, doi:10.1029/2003WR002717.
3. O'Brien, G. S., C. J. Bean and F. McDermott (2003), Numerical investigations of passive and reactive flow through generic single fractures with heterogeneous permeability, *Earth Planet. Sci. Lett.*, 213, 271-284.
4. Hirano, N., N. Watanabe and N. Tsuchiya, (2005), Development of rubber confining pressure vessel and flow test using this apparatus, *J. Min. Mater. Process. Inst. JPN.*, 121, 484-488 (in Japanese with English abstract).
5. Power, W. L. and W. B. Durham (1997), Topography of natural and artificial fractures in granitic rocks: Implication for studies of rock friction and fluid migration, *Int. J. Rock Mech. Min. Sci.*, 34 (6), 979-989.
6. Mourzenko, V. V., J. -F. Thovert and P. M. Adler (1995), Permeability of a single fracture: validity of the Reynolds equation, *J. Phys II France*, 5 (3), 465-482.
7. Tezuka, K. and K. Watanabe (2000), Fracture network modeling of Hijiori hot dry rock reservoir by deterministic and stochastic crack network simulator (D/SC), *Proc. World Geotherm. Cong. 2000*, 3933-3938.
8. Brown, S. R. (1987), Fluid flow through rock joints: The effect of surface roughness, *J. Geophys. Res.*, 92 (B2), 1337-1347.